ОБЪЕДИНЕННЫЙ
ИНСТИТУТ
ЯДЕРНЫХ
ИССЛЕДОВАНИЙ
Дубна

E6 - 3142

D.D. Bogdanov, S. Daroczy, V.A. Karnaukhov,
L.A. Petrov, G.M. Ter-Akopyan

DELAYED PROTON EMITTER ^{111}Te

1967.

E6 - 3142

D.D. Bogdanov, S. Daroczy, V.A. Karnaukhov,
L.A. Petrov, G.M. Ter-Akopyan

DELAYED PROTON EMITTER ^{111}Te

Submitted to ЯФ

I. Introduction

First results of the experiments on the study of delayed proton emitters among tellurium isotopes were presented in papers[1,2]. Furhter on it was shown[3] that the situation with proton emitters in the tellurium region is a little more complicated than it had been described in[1,2]. In the bombardment of separated ^{92}Mo and ^{94}Mo isotopes with ^{20}Ne and ^{22}Ne ions proton activities with half-lives of (4.2 ± 0.2), (19.0 ± 0.7), (13 ± 2) and (60-80) sec[3] were observed. The analysis of the excitation functions drove to a conclusion that the first two emitters are isotopes ^{109}Te and ^{111}Te.

The present work was done with a view of detailed study of the second proton emitter. In our experiments a target of separated ^{102}Pd was bombarded with ^{12}C ions. The experiments were performed with the external beam of the JINR 150 cm Heavy Ion Cyclotron.

II. Experimental Details

A block-diagram of the experimental arrangement is shown in Fig. 1. It was based on the gas collection method developed by Macfarlane and Griffioen[4]. The target[+] was placed before the entrance to a small cy-

[+] The target of ^{102}Pd (1.6 mg/cm^2) was prepared by means of electroplating of a metallic layer on the 3 μ thick copper backing. The isotopic composition was as follows: ^{102}Pd -39.5%; ^{104}Pd -19.0%; ^{105}Pd -20.1%; ^{106}Pd -12.3%; ^{108}Pd -6.4%; ^{110}Pd - 2.2%.

lindrical chamber (stopping chamber) in which helium was applied under pressure of 1 atmosphere. This chamber was connected by means of an orifice (0.35 mm in diam) with a large chamber (detection chamber) which was continuously evacuated. The pressure in the detection chamber was about 1 mm Hg . Because of the large pressure difference a narrow jet of helium poured out of the stopping chamber. Nuclear reaction products were emitted from the target due to the momentum transferred by a projectile, slowed down in helium and taken away by a gas flow. The gas stream was directed to an aluminium catcher. The nuclear reaction products taken away by the gas stream were adsorbed on the surface of the catcher on a spot of about 40 mm^2 (~ 90 per cent of the whole activity adsorbed). The size of the spot was mainly determined by the distance between the catcher and the orifice of the stopping chamber.

The catcher was a disk, 190 mm in diam. It was periodically turned by 45^o away transporting the accumulated activity to a charged particle spectrometer. It took about 0.15 sec to turn the disk. When one sector of the disk was at the spectrometer the neighbouring one gathered activity. The same sector faced the stream every eighth cycle (one complete turn of the disk). This decreased the intensity of the beta-gamma-background, since the long-lived beta activity was uniformly distributed between eight positions.

Helium evacuated from the detection chamber was let through cotton wool filters and then passed back to the stopping chamber. This continuous circulation significantly reduced gas consumption and prevented the danger of radioactive contamination of the air.

In general, the collection efficiency was strongly dependent upon the purity of the gas used. Formerly liquid-nitrogen-cooled traps with activized coal were used for purification of the circulating gas. However, later on it was found that efficient and stable collection can be achieved even without additional purification if the surface of the collector is covered with a thin layer of a high-vacuum silicon oil. In our experiments the collection efficiency was about 50-70%. This value was determined by means of alpha-active dysprosium isotopes which were produced by

the bombardment of Nd with ^{12}C ions. The total activity and its part absorbed on the surface of the catcher from the gas stream were measured simultaneously. For this purpose a grid with known transparency was placed immediately behind the target in the way of the recoils. The total yield was determined by measuring its activity.

The back wall of the stopping chamber was vacuum-sealed with 20 μ thick aluminium foil. The ^{12}C ion beam passed through this foil into a Faraday cup placed in the detection chamber.

In the first experiments a telescope consisting of a thin proportional counter (for measuring $\frac{\Delta E}{\Delta x}$) and a gold-surface-barrier-silicon detector (for measuring E) was used. In these experiments the intensity of alpha emission was very low: $N_\alpha / N_p \leq 0.004$. Therefore later on only a silicon surface-barrier detector was used. The energy resolution of the detector measured by alpha-particles of ThC' was 25-30 keV.

Between the catcher and the spectrometer another disk was placed which could be remotely put in six fixed positions. This disk was used for installation of ^{238}Pu and ThC' calibrating alpha-sources and aluminium absorbers. A 250 μ thick absorber (sufficient to absorb all the protons) was used to determine the background due to intense beta- and gamma-emission and electroinduction.

A spectrometric system designed in the Laboratory of Nuclear Reactions JINR, consisting of a vacuum tube pre-amplifier, semi-conductor amplifier and expander was used in the experiments. Amplitude and time-amplitude analyses were performed by means of AI-256 and AI-4096 analysers. The time of the collection on the cather of the activity was determined by the timer of the analyser. After this period the analyser was blocked and an electromotor was automatically put on to make one turn of the collecting disk. As the activity spot on the catcher approached the spectrometer a photodiod was put in operation. A pulse of the photodiod put off the electromotor and started the analyser. The electronic circuit was also blocked during a high-frequency pulse of the cyclotron.

Results and Discussion

A proton decay curve obtained in the bombardment of ^{102}Pd with ^{12}C ions is shown in Fig. 2. A distinct exponential shape is due to a (19.5 ± 0.5) sec activity.

The proton energy spectra are shown in Figs. 3 and 4. A general behaviour of the proton spectrum is shown in Fig. 3. A sharp rise at lower energy region is due to beta- and gamma-background. A spectrum measured by means of a 0.5 cm^2 surface-barrier detector with a guard ring is shown in Fig. 4. In this case each channel cost about 8 keV.

2. The results of the experiments on measuring the excitation function of the proton emitter are presented in Fig. 5. The ^{12}C ion incident energy was varied by means of absorbers of different thickness. The absorbers were remotely changed during the irradiation. In order to prevent errors due to a possible non-uniformity of the target thickness and the instability of the beam position long-continued bombardments were performed, the incident energy was changed every three minutes and all the points of the curve were consecutively taken. Multiple repetition of these cycles provided for obtaining necessarily averaged data.

The inaccuracy in energy measurements due to a finite thickness of the target and non-monochromacy of the beam was equal to ± 1.5 MeV. The errors in the value of the relative yield are only statistical.

The position of the excitation function maximum for the reaction followed by emission of x neutrons is determined by the following expression:

$$(E_{max})_{cm} = Q_x + \epsilon_x \quad ; \qquad \epsilon_x = 2 \sum_{i}^{x} T_i + E_{\gamma} \quad ,$$

where Q_x is the reaction threshold, T_i is an average temperature in i-evaporation cascade, E_{γ} is the energy taken away by gamma-rays.

In order to calculate the value of $\frac{\epsilon_x}{x}$ the experimental cross sections were normalized over the total cross section calculated according to [5] (the left curve in Fig. 5). The value of Q_x was found

from the mass tables[19] (the mass tables[7,8] give approximately the same values of Q_x). For reactions followed by emission of three and four neutrons the values of $\frac{\epsilon_x}{x}$ are equal, respectively, to:

$$\frac{\epsilon_3}{3} = (6.1 \pm 0.5) \text{ MeV} \quad \text{and} \quad \frac{\epsilon_4}{4} = (2.2 \pm 0.5) \text{ MeV}.$$

The first value is close to the expected one, the second one seems too small[9]. Thus, a 19.5 sec activity can be most probably ascribed to ^{111}Te. This conclusion was later confirmed by the experiments on the study of radioactive properties of ^{111}Te decay products[21].

3. The spectrum shown in Figs. 3 and 4 has a complicated structure. Within an energy range of 2-3.5 MeV there are at least 18 peaks corresponding to transitions between certain levels.

The illustrative scheme of ^{111}Te decay is shown in Fig. 6. The spin - parity of ^{111}Te is probably $5/2^+$ (the spin-parity of the known even-Z nuclei with 59 neutrons is $5/2^+$). Isotope ^{111}Te undergoes beta-transitions to different states of ^{111}Sb. However, the levels corresponding to allowed transitions, i.e. $3/2^+$, $5/2^+$, $7/2^+$ will be populated with greatest probability. The proton binding energy (B_p) in ^{111}Sb is calculated to be about 1.7 MeV[6-8]. That means that ^{111}Sb levels with excitation energy $E^* > 1.7$ MeV are proton-unstable. However, for small values of ($E^* - B_p$) the radiation widths of the levels exceed the proton one due to the effect of the Coulomb barrier. As a result, the yield of protons with energies below 2 MeV is supressed. The relation of the proton width to the radiation one increases with excitation energy. This is the reason of the (average) increase in the intensity of the proton lines within 2-3 MeV energy range. Then the envelope of the proton spectrum goes down due to the reduced level population in beta-transition.

The averaged shape of the proton spectrum can be described by the following expression:

$$N(E_p) = \sum_{i,j} \frac{\Gamma_{pi}^{(j)}}{\Gamma^{(j)}} \rho(E^*, J) W_{(\beta^+ + \epsilon)}(Q_0 - E^*) \quad (1)$$

Here $\rho(E^*,J)$ is the density of the levels with momentum J for a proton-emitting nucleus; $E^* = E_p + B_p + E_i$ is the excitation energy of this nucleus equal to the sum of the proton kinetic energy, the proton binding energy and the excitation energy of the residual nucleus; $\Gamma_{pi}^{(j)}$ is the width of the level with momentum j with respect to the proton emission followed by the formation of a residual nucleus in state i; $\Gamma^{(j)}$ is the total width: $\Gamma^{(j)} = \Gamma_\gamma^{(j)} + \sum_i \Gamma_{pi}^{(j)}$; $W_{(\beta^+ + k)}(Q_0 - E^*)$ is the summarized probability of beta-plus-decay and electron capture in the state with energy E^*; Q_0 is the total electron capture energy.

One can suppose that the spin and energy of the first excited state of ^{110}Sn are 2^+ and ~ 1.2 MeV (similarly to other even isotopes $^{112-118}Sn$). Then the greatest contribution to the proton energy spectrum is made by decays in the ground state of ^{110}Sn; the contribution of transitions to excited states is very small (only several per cent). The transitions from the level $7/2^+$ to the ground state of ^{110}Sn are significantly suppressed due to the proton centrifugal barrier ($\ell_p = 4$). Therefore the proton spectrum is mainly determined by the transitions from the levels $3/2^+$ and $5/2^+$.

The proton level widths in the formula (1) were calculated from the known statistical formula[10]:

$$\Gamma_{pi}^{(j)} = \frac{(2s+1)(2i+1)(2\ell+1)}{2\pi\rho(E^*,j)} P_p^{(\ell)}(E_p). \qquad (2)$$

Here s is the proton spin, ℓ is the proton orbital momentum, i is the spin of the final state (^{110}Sn). The penetration factors $P_p^{(\ell)}(E_p)$ were taken from paper[11]x/. The radiation widths were calculated from a semi-empirical formula for the dependence of $\Gamma_\gamma^{(j)}$ upon the excitation energy, mass number and level density[12]. The level density $\rho(E^*,j)$ for ^{111}Sb was calculated from the data of Gilbert and Cameron[13]. The calculated values of $\frac{\Gamma_p}{\Gamma}$ of the levels $5/2^+$ for different B_p values are shown in Fig. 7.

The probability of beta-plus-transition $W_{(\beta^+ + k)}(Q = E^*)$ in formula (1) can be written as follows:

---

x/ The authors are grateful to B.I.Pustylnik for some calculations of the penetration factors.

$$W_{(\beta^+ + k)}(Q_0 - E^*) = F(Q_0 - E^*)\, M^2(E^*), \qquad (3)$$

where $F(Q_0 - E^*)$ is the known function of energy determined by the nomograms for the transitions of beta-plus-decay and electron capture [14]. $M^2(E^*)$ is the averaged squared matrix element of beta-plus-transition. Its exact dependence upon excitation energy is unknown. The analysis of data on the probability of delayed neutron emission (for example. in [15]) is usually performed on the assumption that M^2 = const, i.e. is insensitive to the excitation energy of the daughter nucleus. At the same time there are indications that the matrix element of beta-transition is probably inclined to decrease with increasing level densities of the daughter nucleus [16].

The proton spectra calculated from formula (1) on the assumption that M^2 = const is shown in Fig. 8 together with the averaged experimental spectrum. One can state that the calculated results do not agree with the experimental ones for any permissible values of B_p and Q_0. The change of values B_p and Q_0 as compared with those given in Fig.8 lead to even greater disagreement. This disagreement cannot be explained by errors in calculating values of $\frac{\Gamma_p}{\Gamma}$. One can only admit that the matrix element of beta-transition sharply reduces with increasing excitation energy of ^{111}Sb.

The theoretical curve satisfactorily describes the averaged shape of the proton spectrum on the assumption that $M^2\rho$ = const. The results of the calculations are given in Fig. 9. The shape of the spectrum to the right of the maximum permits to determine the maximum proton energy $E_{p\,max} = Q_0 - B_p$; the position of the maximum is sensitive to the values of B_p, Γ_p, Γ_γ. The best agreement is achieved for $Q_0 - B_p = 5$ MeV. The accuracy of the determination of the value B_p is not high due to possible errors in calculations of the absolute values of Γ_p and Γ_γ (especially at proton energies below 3 MeV). The values of B_p, Q_0 and $E_{n\,max} = Q_0 - B_n$ obtained by the comparison between the experimental and the calculated spectra are given in Table I. The corresponding values obtained from different semi-empirical mass formulae [6-8;17-19] are also shown.

It is noteworthy that our results agree with calculations from the Garvey-Kelson relation[20] and are close to predictions from the semi-empirical formula of Zeldes et al.[19].

Further study of delayed proton spectra seems interesting since it can give information on $M(E^*)$, $\frac{\Gamma_p}{\Gamma}$ proton binding energy and the energy of beta-plus-decay of certain nuclei.

The authors are grateful to Professor G.N.Flerov, Corresponding Member USSR Academy of Sciences, for permanent and encouraging interest and useful discussions. The authors thank V.F.Kushniruk and Yu.P.Kharitonov for preparing high-resolution silicon surface-barrier detectors and to V.G.Subbotin and B.V.Fefilov for designing spectrometric devices.

Table I

	Experimental	Cameron [6]	Seeger [7]	Swiatecki and Myers [8]	Wing and Varley [17]	M.Hillman [18]	Zeldes, Gronau and Lev [19]	Garvey and Kelson [20]
^{111}Te	6.3–6.9	8.3	7.57	7.89	5.73	5.86	6.96	6.7
Q_{0} MeV ^{111}Sb	1.3–1.9	1.59	1.59	1.75	3.24	2.8	2.13	1.7
B_p MeV								
$E_{p\,max}$ = $= Q_0 - B_p$	$4.9 < E_{p\,max} \leq 7.22$		6.49	6.65	3.0	4.1	5.34	5.0
	≤ 5.3							

References

1. V.A.Karnaukhov, G.M.Ter-Akopyan, L.A.Petrov, V.G.Subbotin. Yadernaya Fizika, 1, 812 (1965).
2. A.T.Siivola. Phys.Rev.Lett., 14, 142 (1965).
3. V.A.Karnaukhov, G.M.Ter-Akopyan, L.S.Vertogradov, L.A.Petrov. Yadernaya Fizika, 4, 457 (1966). Preprint P-2514, Dubna, 1965.
4. R.D.Macfarlane, R.D.Griffioen. Nucl.Instr.Meth., 24, 461 (1963).
5. V.V.Babikov. Preprint P-1351, Dubna, 1963.
6. A.G.W.Cameron. At.Energy Can. Ltd. Rept. CRL-41 (1957).

7. P.A.Seeger. Preprint LA-3380-MS (1965).
8. W.D.Myers, W.J.Swiatecki. Preprint UCRL-11980 (1965).
9. J.M.Alexander, G.N.Simonoff. Phys.Rev., 133, B104 (1964).
10. V.F.Weisskopf, D.H.Ewing. Phys.Rev., 57, 472 (1940).
11. G.S.Mani, M.A.Melkanoff, J.Jori. Report CEA 2379 (1963).
12. A.Stolovy, J.A.Harvey. Phys.Rev., 108, 353, (1957).
13. A.Gilbert, A.G.W.Cameron. Can. J.Phys., 43, 1446 (1965).
14. A.H.Wapstra, G.I.Nilch, R.Van Lischut. Tables on Nuclear Spectroscopy, Atomizdat, Moscow, 1960.
15. G.P.Keepin, J. of Nuclear Energy, 7, 13 (1958).
16. B.Mottelson. Private Communication, 1966.
17. J.Wing, J.D. Varley. Preprint ANL-6886.
18. M. Hillman. Preprint BNL 846 (T-333).
19. N.Zeldes, M.Gronau, A.Lev. Nuclear Physics, 63, 1 (1965).
20. G.T.Garvey, I.Kelson. Phys.Rev.Lett., 16, 197 (1966).
21. D.D.Bogdanov, J.Bacso, V.A.Karnaukhov, L.A.Petrov. Preprint P6-3138. Dubna, 1967.

Received by Publishing Department
on January 26, 1967.

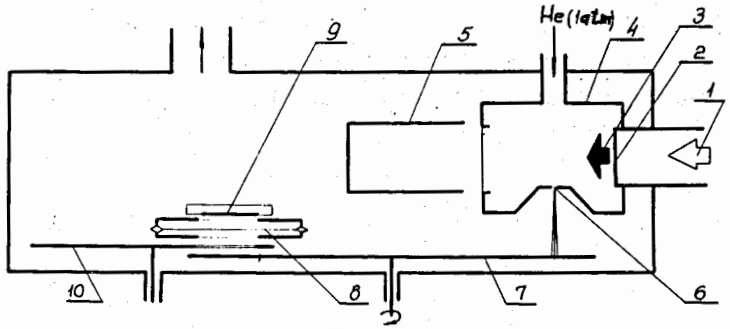

Fig. 1. The layout of the experimental arrangement. 1 - ^{12}C ion beam, 2 - target, 3 - recoils, 4 - stopping chamber, 5 - Faraday cup, 6 - orifice, 7 - recoil catcher, 8 - gas counter ($\Delta E/\Delta x$), 9 - surface-barrier detector, 10 - disk for mounting absorbers and calibrating alpha-sources.

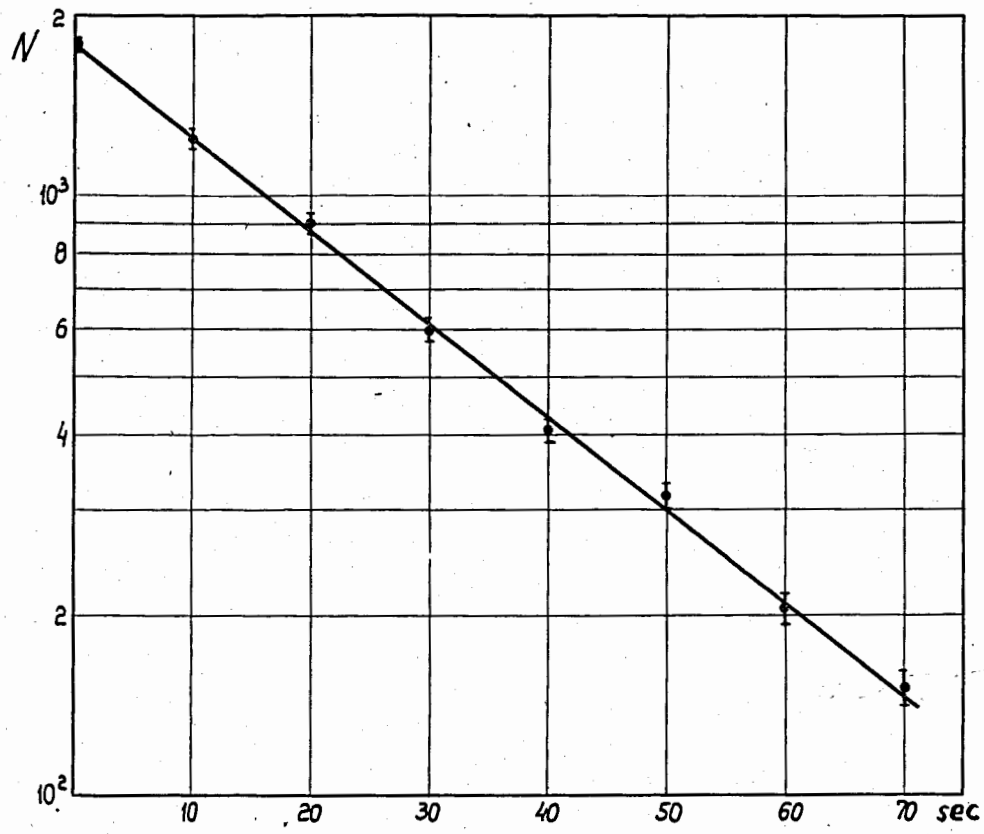

Fig. 2. The decay curve of p -activity from the reaction $^{102}Pd+^{12}C$.

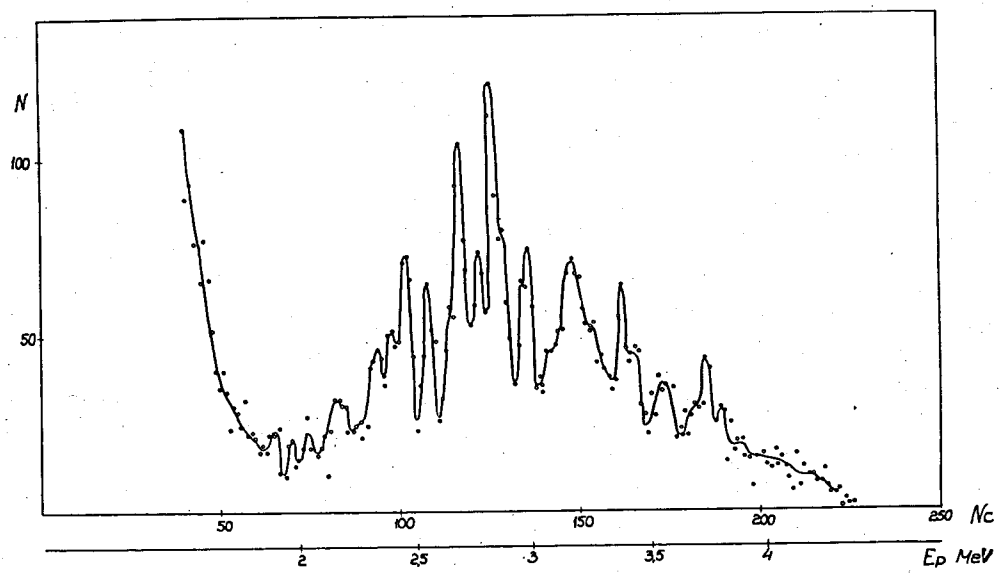

Fig. 3. The spectrum of a 19.5 sec proton emitter taken with resolution of 50–60 keV.

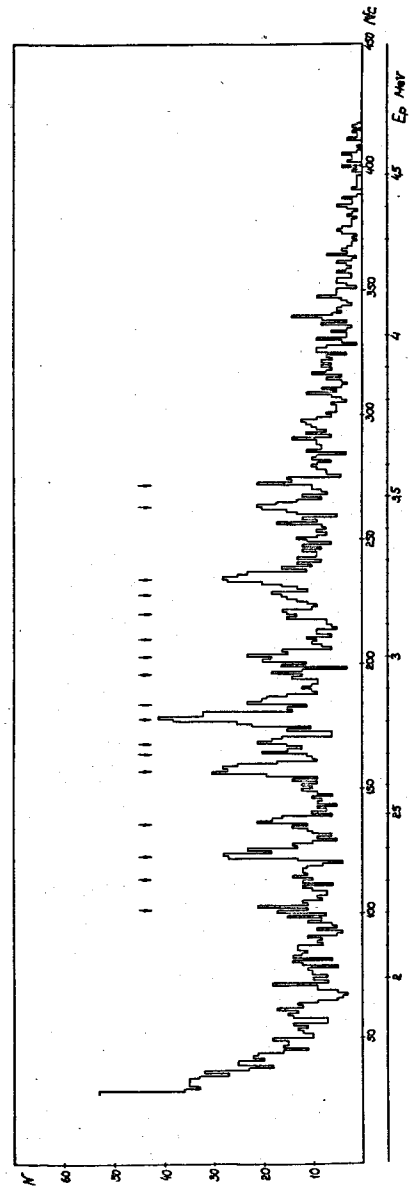

Fig. 4. The spectrum of a 19.5 sec proton emitter taken with resolution of 25–30 keV.

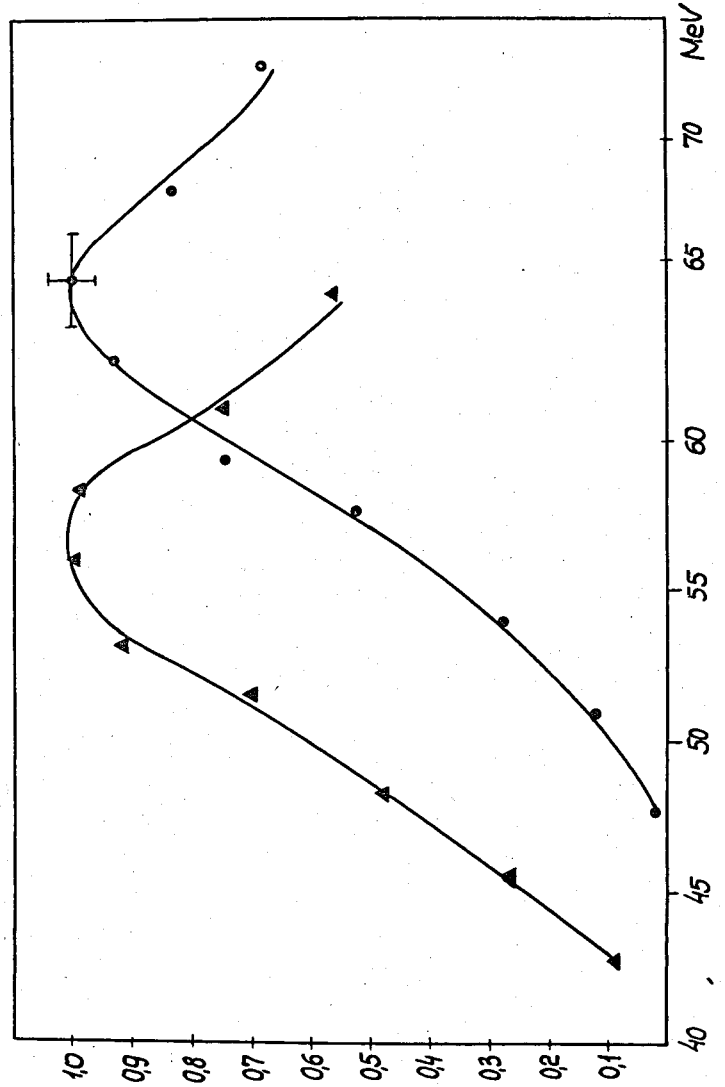

Fig. 5. Excitation function of a 19.5 sec proton emitter.

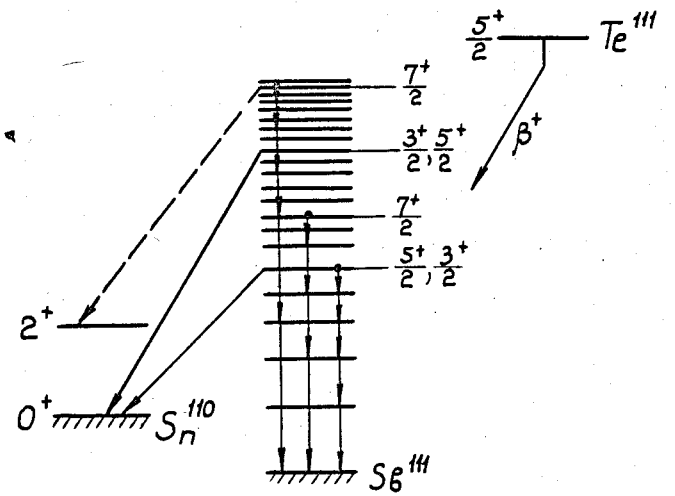

Fig. 6. The illustrative scheme of ^{111}Te decay.

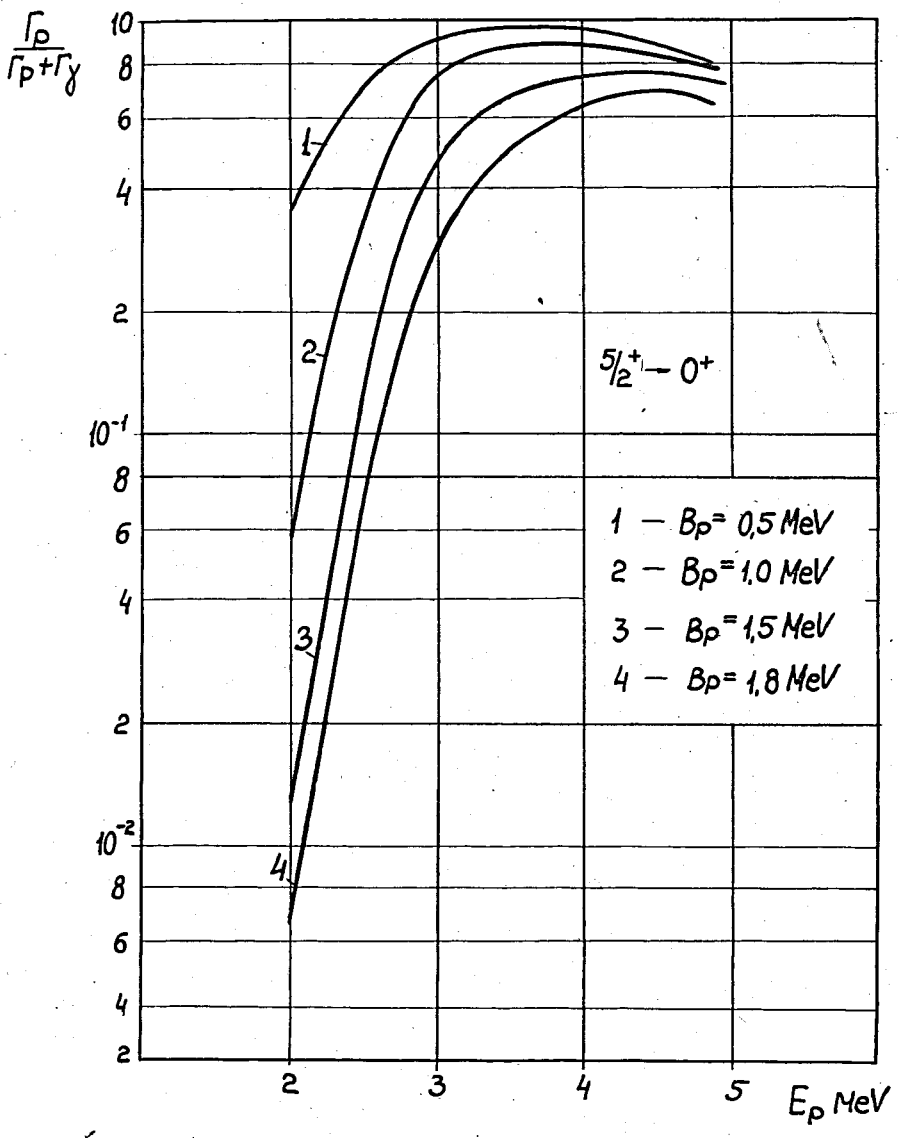

Fig. 7. The calculated values of Γ_p / Γ for the levels $5/2^+$ of ^{111}Sb for different values of B_p.

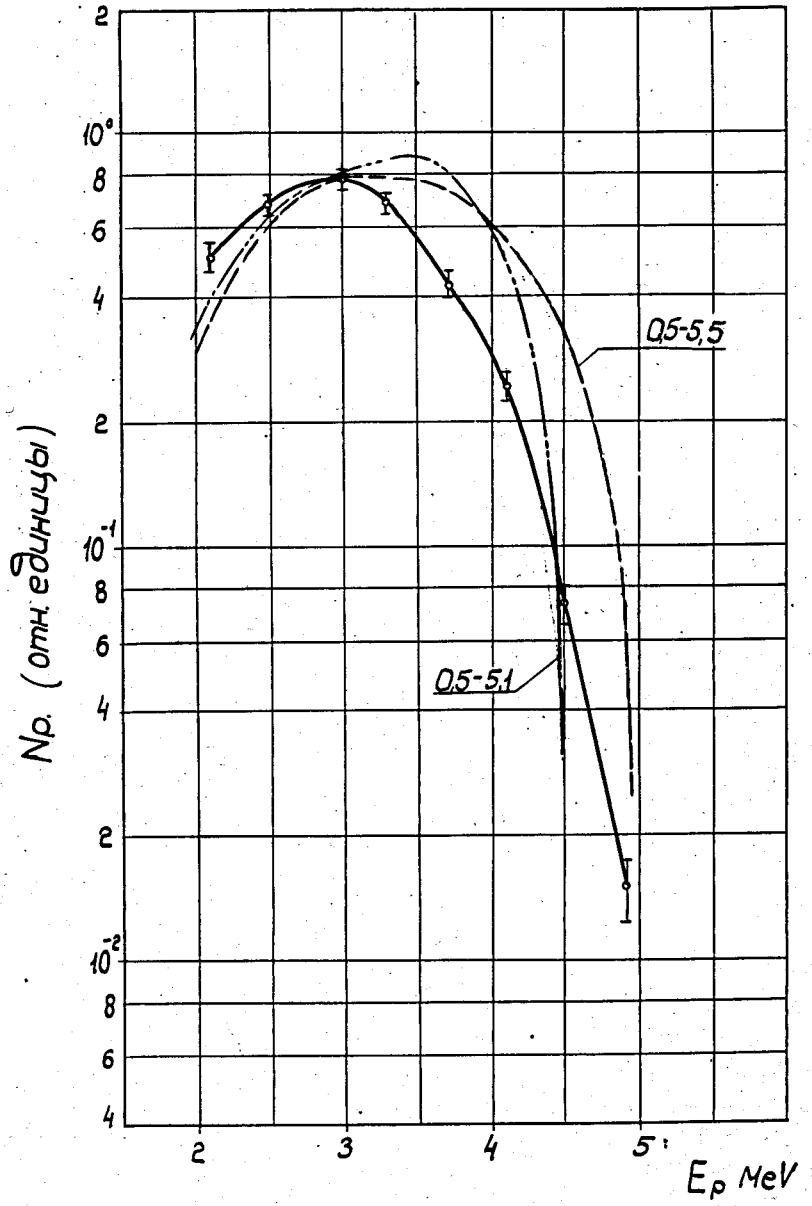

Fig. 8. The comparison of the calculated proton energy spectrum with the averaged experimental one on the assumption that M^2 = const.

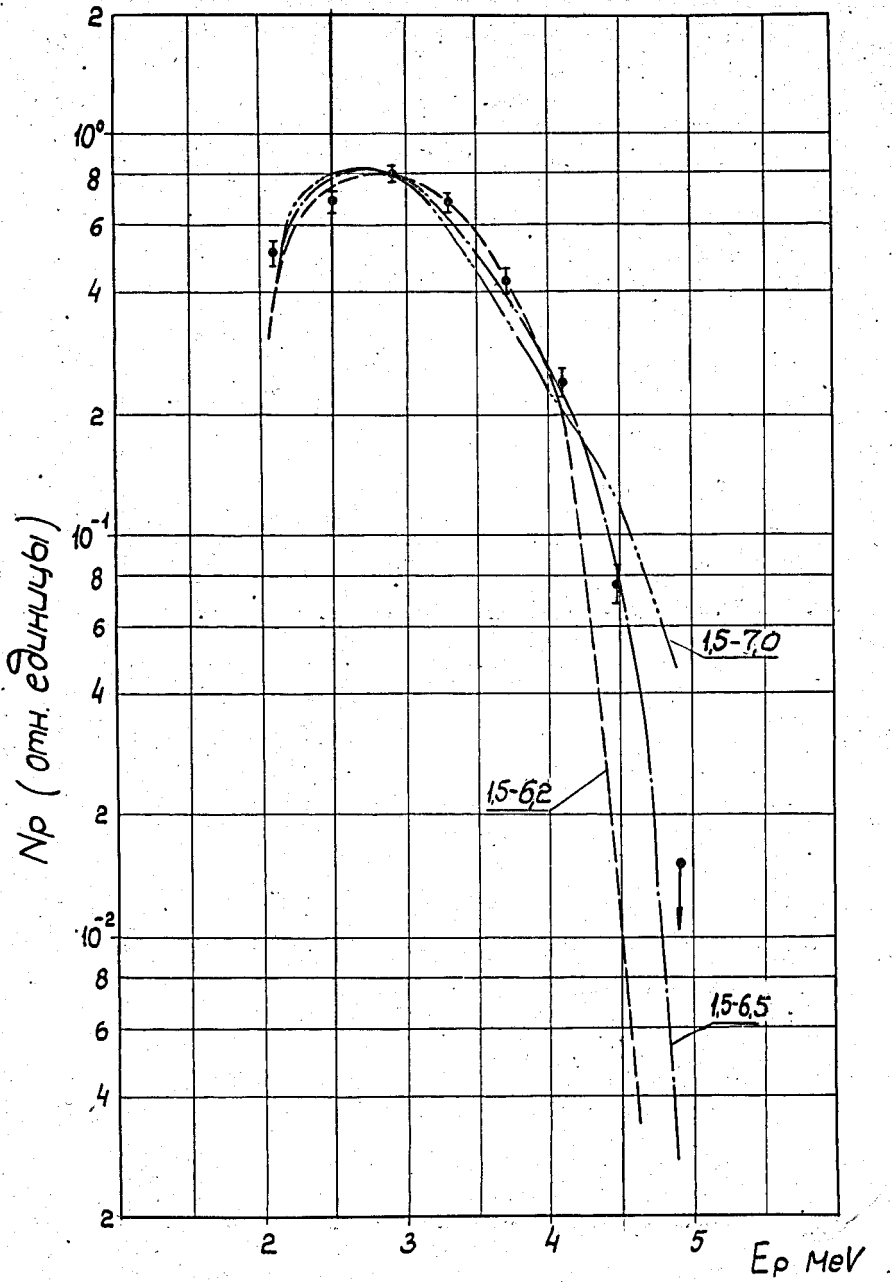

Fig. 9. The comparison of the calculated proton energy spectrum with the averaged experimental one on the assumption that $M^2\rho$ = const.